

# Improving cerebral blood flow quantification for arterial spin labeled perfusion MRI by removing residual motion artifacts and global signal fluctuations

Ze Wang\*

*Department of Psychiatry, Perelman School of Medicine, University of Pennsylvania, Philadelphia, PA 19104, USA*

*Department of Bioengineering, School of Engineering and Applied Science, University of Pennsylvania, Philadelphia, PA 19104, USA*

Received 10 October 2011; revised 12 April 2012; accepted 14 May 2012

---

## Abstract

Denoising is critical to improving the quality and stability of cerebral blood flow (CBF) quantification in arterial spin labeled (ASL) perfusion magnetic resonance imaging (MRI) due to the intrinsic low signal-to-noise-ratio (SNR) of ASL data. Previous studies have been focused on reducing the spatial or temporal noise using standard filtering techniques, and less attention has been paid to two global nuisance effects, the residual motion artifacts and the global signal fluctuations. Since both nuisances affect the whole brain, removing them in advance should enhance the CBF quantification quality for ASL MRI. The purpose of this paper was to assess this potential benefit. Three methods were proposed to suppress each or both of the two global nuisances. Their performances for CBF quantification were validated using ASL data acquired from 13 subjects. Evaluation results showed that covarying out both global nuisances significantly improved temporal SNR and test-retest stability of CBF measurement. Although the concept of removing both nuisances is not technically novel per se, this paper clearly showed the benefits for ASL CBF quantification. Dissemination of the proposed methods in a free ASL data processing toolbox should be of interest to a broad range of ASL users.

© 2012 Elsevier Inc. All rights reserved.

**Keywords:** Arterial spin labeling; Motion correction; CBF; Global signal; Test-retest stability; Temporal SNR

---

## 1. Introduction

Arterial spin labeled (ASL) perfusion magnetic resonance imaging (MRI) is a noninvasive technology to measure cerebral blood flow (CBF) using the magnetically labeled arterial blood water as an endogenous tracer [1,2]. Limited by the T1 decay of the labeled spins and the transit time from the labeling plane to the imaging place, the labeling time in ASL perfusion MRI is usually around 1–2 s. As a result, the total labeled blood flow is less than one percent of the static water in the imaging location; so that ASL perfusion signal only accounts for approximately one percent of the mean MR signal intensity [3] in the absence of background suppression [4]. This problem is even more acute in the case

of functional studies since the functional activation-induced ASL signal change generally only accounts for a few tenths of this small fraction of baseline signal change. Therefore, any baseline signal fluctuations can easily overwrite this small percentage change. In time series MRI like functional MRI (fMRI), head motions can not be fully corrected from the data. There always exist residual motion effects [5]. ASL CBF is derived from signal changes between arterial labeling and control labeling and are therefore highly sensitive to head motion [6], not only the motion at each time point but also the relative motion between the control image and the label image within each L/C image pair [6]. Therefore, suppressing residual motions is important to improve the subsequent CBF quantification. Previous studies have been focused on suppressing noise in ASL data using different ASL signal models [7–9], spatial smoothing [10,11], temporal filtering [8,12], outlier cleaning [6,13] or some image-based denoising methods [14,15], less attention has been paid to the residual motion artifacts and the global

---

\* Treatment Research Center, University of Pennsylvania, Philadelphia, PA 19104, USA. Tel.: +1 215 222 3200 123; fax: +1 215 386 6770.

E-mail address: [zewang@mail.med.upenn.edu](mailto:zewang@mail.med.upenn.edu).

signal fluctuations. Because of the motion estimation errors and the precisions of the subsequent single interpolations of any motion correction (MoCo) method, residual motions are always there. Global signal fluctuations are inevitable as well due to the temporal MR signal variations, thermal noise, or physiological variations.

Removing the residual motion artifacts has been a standard signal processing step in the blood-oxygen-level-dependent (BOLD) contrast-based functional MRI since the early work by Friston et al. [5] but has not been explicitly assessed in ASL MRI. Removal of whole brain global signal has long been discussed in the BOLD fMRI literature [16–19], but still not explicitly addressed in ASL MRI. In ASL MRI, the global signal fluctuations can be effectively suppressed using standard signal filtering if we know the bandwidth range. However, the global MR signals could vary differently across scan time or subjects, resulting in a difficulty of defining an optimal cutoff frequency for the filter to be used. Global signal provides a data-derived estimation for this global change, and regressing it out from ASL data provides an easy way to clear up this type of nuisance effects.

The purpose of this study was to assess the efficacy of removing these two nuisance variables for ASL CBF quantification. A new ASL MoCo method was first proposed to simultaneously correct head motions and prevent taking the systematic label/control signal difference as an apparent motion term [6]. The estimated motion time courses and the whole brain global signal were orthogonalized to the oscillating label/control paradigm and were then regressed out from the ASL image series before CBF quantification. Test-retest resting ASL data were collected to evaluate the efficacy of these methods for CBF quantification as compared to standard ASL CBF quantification routine.

## 2. Materials and Methods

### 2.1. Subjects

Thirteen young healthy subjects (mean age=25.04±3.92, 7 male) were scanned twice with 1.5 to 2 months apart with signed written consent forms approved by the local institutional review board.

### 2.2. Image acquisition

MRI was conducted in a Siemens 3T Trio whole-body scanner (Siemens Medical Systems, Erlangen, Germany). ASL images were scanned using an amplitude modulated continuous ASL (CASL) perfusion imaging sequence optimized for 3.0 T [20] with a standard transmit/receive (Tx/Rx) head coil (Bruker BioSpin, Madison, WI, USA). The head coil and foam pads were positioned carefully to reduce movement. Acquisition parameters were TR=3.8 s, TE=17 ms, FOV= 220×220 mm<sup>2</sup>, matrix=64×64×12, slice thickness=7 mm, inter-slice space=2.35 mm, labeling

time=2 s, post label delay time=1 s, bandwidth=3 kHz/pixel, flip angle=90°. Fifty label/control image pairs were acquired for each subject. Participants were asked to lie still in the scanner at rest and keep eyes open.

### 2.3. A simplified ASL MRI MoCo method

The rigid-body transformation-based MoCo method [5,21] as implemented in SPM (<http://www.fil.ion.ucl.ac.uk/spm/>) was amended for ASL data motion correction. Three substeps were involved. First, all ASL images, including all label images and control images in the original acquisition order were input to the standard MoCo procedure and the 3 translational and 3 rotational motion time courses were estimated for the entire ASL image series. Second, the zig-zagged label-control patterns were regressed out from those motion time courses through simple regressions. Denoting label by −1 and control by 1, the zig-zagged label-control paradigm is a binary numerical series consisting of oscillating −1 and 1. Third, the cleaned motion parameters were then used for real MoCo. With this amendment, separate MoCos for the label images and control images [6] are no longer required. This modification has been included in the latest version of ASLtbx [6] which is freely available at <http://cfm.upenn.edu/~zewang/ASLtbx.php>.

### 2.4. Other data preprocessing

Other data processing was also performed using the SPM (<http://www.fil.ion.ucl.ac.uk/spm/>) based batch scripts provided in ASLtbx [6]. Spatial smoothing was conducted using an isotropic Gaussian filter with a full width at half maximum of 5 mm<sup>3</sup>. Temporal filtering was performed using a high-pass Butterworth filter (cutoff frequency=0.01 Hz). Image mask was generated by thresholding the mean image with a threshold of 20% of the maximum intensity of the mean image. This mask was used to remove extracranial voxels for calculating the global signal.

### 2.5. A general linear model (GLM) for ASL CBF quantification

GLM is a natural model for regressing out confounds from time series, and has long been used since the inception of BOLD fMRI. It has also been adapted in ASL MRI for confound removal [22,23] and for CBF quantification in Ref. [24]. Using a GLM, perfusion weighted signal modulation and the subsequent CBF quantification in ASL MRI can be described with [24]:

$$\mathbf{y} = [\mathbf{x}_{ideal}\mathbf{x}_{var}][\beta_{ideal} \beta_{var}] + c + \varepsilon \quad (1)$$

where  $\mathbf{y}$  is the preprocessed ASL time series at a certain voxel,  $\mathbf{x}_{ideal} = [-0.5, 0.5, \dots, -0.5, 0.5]^T$  is the ideal labeling paradigm for the alternative label control ASL data acquisitions (the signs for −0.5 and 0.5 should be changed if the image acquisition order is control-label-control-label),  $\mathbf{x}_{var}$  (var means variation) is for modeling temporal nuisances

such as the residual motions and global signal fluctuations,  $\beta_{ideal}$  and  $\beta_{var}$  are the fitting coefficients for  $x_{ideal}$  and  $x_{var}$ , respectively,  $c$  is the mean of  $y$  and  $\varepsilon$  is the fitting error. Using this model, two approaches can be used to calculate the underlying CBF value. One is to take  $\beta_{ideal}$  as the perfusion signal difference  $\Delta M$ . For CASL, the constant  $c$  in Eq. (1) can be used as the baseline MR signal  $M_0$ , and CBF can be calculated with  $f = \frac{\beta_{ideal} \lambda R_{1a} \exp(\omega R_{1a})}{2c\alpha} [1 - \exp(-\tau R_{1a})]^{-1}$ , where  $f$  is CBF,  $R_{1a}$  is the longitudinal relaxation rate of blood,  $\tau$  is the labeling time,  $\omega$  is the post labeling delay time,  $\alpha$  is the labeling efficiency and  $\lambda$  is blood/tissue water partition coefficient [25]. For pulsed ASL CBF quantification, we can still use  $\Delta M = \beta_{ideal}$ , and  $c$  should be replaced by  $M_0$  which is generally acquired separately. The other approach is to remove the nuisance effects from the acquired data using the following approximation:

$$\hat{y} = x_{ideal} \beta_{ideal} + c + \varepsilon \quad (2)$$

and then use these nuisance-cleaned control/label images to calculate CBF as usual. The second approach was used in the following experiments because it can output the CBF map series, which are needed to calculate the temporal signal-to-noise ratio (TSNR) for CBF quantification.

#### 2.6. Removing residual motion artifacts and global signal fluctuations

Motion time course (three translations and three rotations) and/or the global signal after orthogonization with respect to the ideal label/control paradigm were included in  $x_{var}$  in Eq. (1). Then Eq. (2) was used to generate the nuisance-cleaned ASL data  $\hat{y}$ .

#### 2.7. CBF quantifications using four different approaches

After the same preprocessing as described above, CBF images were calculated using four different methods. Method 1 was the standard simple subtraction-based CBF calculation without nuisance correction (NoNu). Methods 2, 3 and 4 were based on nuisance-cleaned ASL data  $\hat{y}$ . Method 2 removed the residual motion effects before CBF calculations by including the orthogonized motion time courses as the nuisances in Eq. (1) (NuMot); Method 3 removed the global fluctuations before CBF calculations by including the global signal as the nuisance in Eq. (1) (NuGS); both residual motions and global fluctuations were included as nuisances in Eq. (1) in Method 4 (NuMotGS).

#### 2.8. Performance indices

TSNR was calculated from the CBF image series generated by each of the 4 methods (TSNR = mean of the time series / standard deviation of the time series). The TSNRs of NuMot, NuGS and NuMotGS were divided by that of NoNu to directly show the TSNR increase due to the removal of the two global nuisances. The TSNR ratio was then averaged across the whole brain as an aggregate performance index.

The second performance index collected in this paper is the within-subject CBF measurement test-retest stability. The whole brain CBF was calculated by averaging all the intracranial voxels' CBF values, and the same group of subjects' whole brain mean CBFs of Scan 1 was then correlated to those of Scan 2.

#### 2.9. Correlation between mean TSNR and mean CBF

Since the spectrum of ASL perfusion signal tends to be flat [7], the noise in the subtracted ASL perfusion data tends to be white noise. Therefore, any temporal nuisance removal should bring the perfusion signal to be more Gaussian distributed. Resultantly, TSNR, which is equal to the ratio of mean and standard deviation, should be more closely related to the mean CBF value after nuisance removal, and this correlation can retrospectively indicate the efficacy of the proposed nuisance removal methods. To verify this possible relationship, the correlation between the whole-brain mean TSNR and the whole-brain mean CBF was calculated for each of the four assessed methods.

### 3. Results

#### 3.1. TSNR performance of removing global nuisances for CBF quantification

Fig. 1 shows the whole brain mean TSNR increase of the nuisance-removal-based CBF quantification methods as compared to NoNu. NuMot, NuGS and NuMotGS yielded significant TSNR improvement as compared to NoNu for both scans (Fig. 1A and Fig. 1B) (one-sample  $t$  test for testing the mean increase against 0,  $P \leq .00013$ ), and the mean whole brain TSNR increment was greater than 14.74%, 8.01% and 17.93%, respectively. Fig. 1C further shows that the TSNR improvement obtained by removing the global nuisances was consistent across scan time ( $P < .004$  for all the linear fitting lines). Fig. 2 shows the TSNR maps of a typical subjects' ASL CBF series calculated using the 4 assessed quantification routines: NoNu, NuMot, NuGS and NuMotGS. As compared to NoNu (Fig. 2A), removing global nuisances improved TSNR nearly in the whole brain. Particularly, removing residual motion effects markedly improved TSNR in the sinus region as shown in the first 2 slices in Fig. 2B and 2D.

Table 1 lists the correlation coefficients (CCs) of the mean TSNR vs. mean CBF for all four methods. Either covarying out the residual motion effects or the global fluctuations yielded higher correlations between TSNR and CBF; removing both temporal nuisances yielded the highest correlation between whole brain TSNR and whole brain CBF.

#### 3.2. Test-retest stability of CBF quantification

Fig. 3 shows the correlation of the whole brain mean CBF values at the 2 scan sessions. The inter-session CBF CCs of the four assessed methods, NoNu, NuMot, NuGS and NuMotGS, were 0.38 ( $P = .2$ ), 0.56 ( $P = .047$ ), 0.59 ( $P = .033$ ),

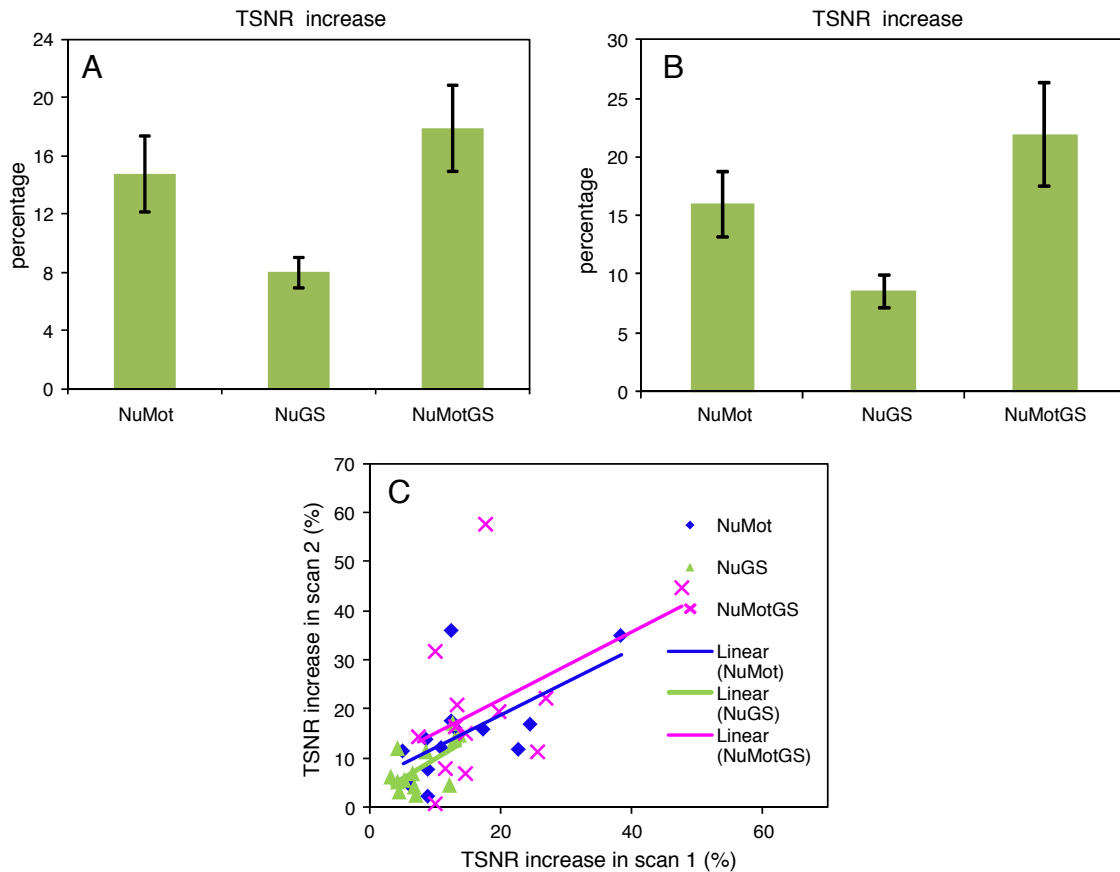


Fig. 1. TSNR performance of the global nuisance removal-based CBF quantification methods as compared to the standard CBF quantification approach. (A) TSNR increases of the proposed methods for ASL data acquired at Time 1. (B) TSNR increases of the proposed methods for ASL data acquired at Time 2. (C) Time 1 vs. Time 2 TSNR increases. The percentage of increase is based upon the TSNR value of standard ASL CBF quantification without removing either of the two global nuisances.

0.54 ( $P=.05$ ), respectively. Removing global nuisance improved the test–retest stability of the global CBF measurement using ASL MRI.

### 3.3. CBF maps

Fig. 4 shows the subject's CBF images calculated using the 4 methods. Spatial smoothing was not applied to the motion corrected data in order to have a better visualization of the image quality difference between the methods with and without corrections for the nuisance variables. The color map is from 0 to 100 ml/100 g per minute. As compared to NoNu (Fig. 4A), all methods with nuisance corrections showed improved image quality in regions as marked by the sky blue arrows, in terms of fewer voxels in orbitofrontal, bilateral temporal, anterior cingulate and posterior cingulate showing extremely large CBF values and fewer voxels in the prefrontal cortex (the right two slices) showing close to zero or negative CBF values (the dark regions).

## 4. Discussion

Post-processing represents a promising way to improve ASL CBF quantification. Three ASL signal processing

methods were presented in this paper to remove either one (NuMot, NuGS) or both (NuMotGS) of the two global nuisances that are inevitable in ASL MRI: the residual motion artifacts and the global signal fluctuations. Evaluations using repeat ASL scans from 13 normal healthy people demonstrated better CBF quantifications in terms of higher temporal SNR, better test–retest stability and better CBF map quality.

Due to the imperfection of signal interpolations in MoCo and motion-induced spin excitation history [5], head motions can not be fully corrected. It is then desirable to suppress them before CBF calculation to prevent noise propagation of the residual motion artifacts, which could even be amplified during the control minus label image subtraction step in ASL CBF quantification. Our data clearly showed that regressing out the residual motion effects improved the stability of CBF measurement.

Global signal fluctuations can not be effectively suppressed using standard signal filtering due to the difficulty of defining an optimal cutoff frequency. Regressing out the global signal provides an easy way to clear up this type of nuisance effects. Removal of global signal however does not exclude regular filtering. A high-pass filtering was used to



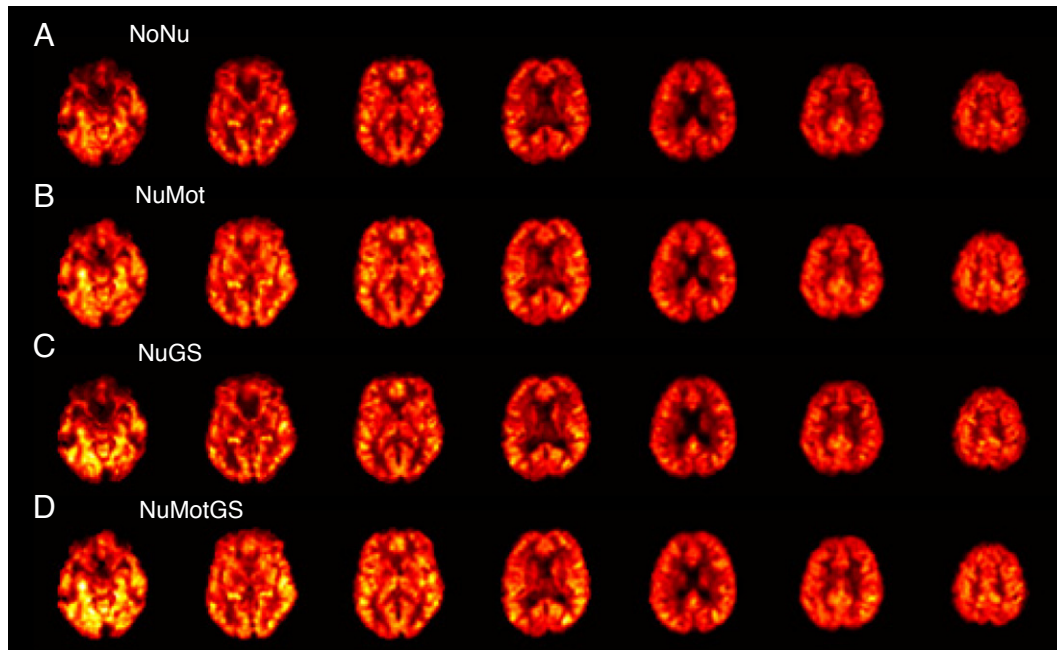


Fig. 2. TSNR maps of a typical subject's ASL CBF series calculated using different approaches as marked by the label on top of each row in the figure. The display window is from 0 to 4.

remove the low frequency part of the MR signal fluctuations before any further analysis. Even based upon that preprocessing, our data still showed CBF quantification quality improvement by regressing out the global fluctuations. Removing global signal has been skeptical in BOLD fMRI due to the possibility of introducing apparent anti-correlations [26–28]. However, this possibility should not exist in ASL MRI where the perfusion signal of interest is generally obtained from the difference between the successive control and label images. Since the global signal is orthogonalized to the zig-zagged spin labeling paradigm, removing global signal before subtraction should not affect the underlying perfusion signal except suppressing the noise. Consequently, the correlation coefficient distribution shift [28] due to the removal of global signal in the control/label images should not occur to the perfusion signal, since the successive subtraction is approximately a differentiation process. Theoretically, one cannot prove that the sum of correlations between a source region and the rest of brain using the subtracted perfusion data will be less than or equal to 0 (Eqs. 7 and 8 in Ref. [28]).

Our data (Figs. 1 and 2) showed that removing residual motion effects (NuMot) yielded higher TSNR than taking the global fluctuations out (NuGS). A possible reason might be

that part of the global fluctuations have already been canceled out during the control-label subtraction even the global signal is not included as a nuisance variable in the residual motion removal-based CBF quantification. Nevertheless, our data also showed that removing both nuisance variables (NuMotGS) yielded further temporal stability and test-retest stability of ASL CBF measurement. Since a T2\*-weighted gradient-echo echo planar imaging sequence was used to acquire the ASL images in this paper, MR signal in the sinus regions had large difference across voxels due to

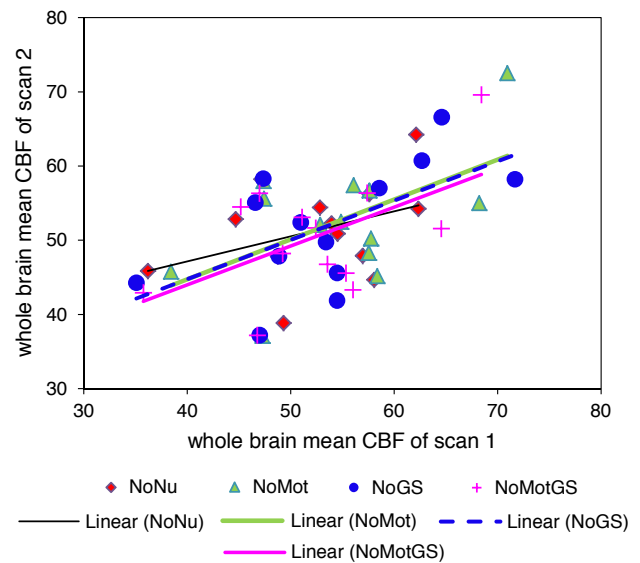


Fig. 3. Removing global nuisance variables improved the stability of whole brain mean CBF measured using ASL MRI at two scan times.

Table 1  
Correlation between TSNR and whole brain mean CBF

Method	NoNu		NuMot		NuGS		NuMotGS	
	CC	P	CC	P	CC	P	CC	P
Scan1	0.5	.08	0.57	.042	0.56	.05	0.61	.026
Scan2	0.58	.011	0.69	.0086	.68	0.0104	0.79	.0012

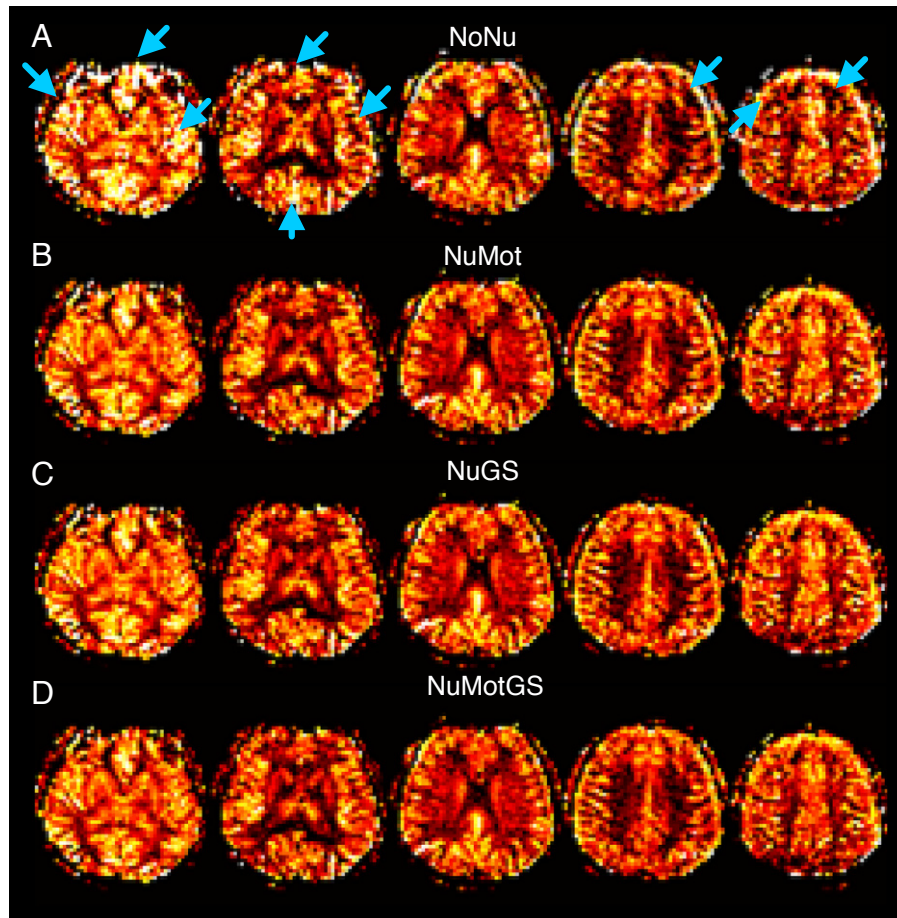


Fig. 4. A representative subject's CBF maps calculated with different ASL CBF quantification methods: (A) NoNu, (B) NuMot, (C) NuGS and (D) NuMotGS. The display window for mapping image intensity is from 0–100 ml/100 g/min.

the large susceptibility gradients in that area. Any residual temporal misalignment could result in amplified artifacts due to the spatial signal difference across neighboring voxels. Removing the residual motion effects could then substantially improve the stability of CBF quantification in that region as demonstrated in Fig. 2. Although not clearly demonstrated, this potential benefit could occur to the peripheral brain regions due to the spatial MR signal difference across the neighboring voxels in those regions as well.

Removing residual motions (NuMot), global fluctuations (NuGS) and both nuisances (NuMotGS) improved the whole brain CBF test-retest stability in terms of higher inter-scan CBF correlations (Fig. 3). As CBF is a relatively stable physiological measure, these results showed that removing the global temporal artifacts reduced the variations of ASL CBF measurement. The correlation coefficient between the global CBF of two scans was less than 1, which might reflect two limitations of the acquired data: one is that the sample size was small, the other is that the time interval between two scans was relatively long and the physiological CBF measurement variations could be large. Nevertheless, our data showed that the proposed methods would be useful for

using ASL to assess any longitudinal CBF effects by reducing the overall temporal variations.

Our results also showed that removing these global nuisances improved the correlation between whole brain mean CBF and whole brain mean TSNR, meaning that the temporal nuisances account for a large extent of the perfusion signal variations. Since the TSNR is calculated via dividing the standard deviation from the mean of the CBF value, higher CBF vs. TSNR correlation corresponds to smaller across-subject variations of the temporal CBF variance, meaning that removing the two nuisances stabilized CBF quantification across subjects.

It is worth to note that removing both motion artifacts and global fluctuations is not novel in fMRI field per se. It has long been established in BOLD fMRI data processing. Similar approaches have also been proposed in ASL MRI. However, no one has explicitly shown the benefit of removing both nuisances. Our data provided the first evidence to this endeavor. A limit of this study is that we didn't acquire physiological data including cardiac signal and respiratory signal so we could not retrospectively clean up these physiological noises from the ASL data. Since a CASL sequence was used to acquire the ASL data, minor

variations due to the physiological interference were expected to be occurred to the CBF quantification due to the long spin labeling duration used in CASL acquisition [29]. But surely, removing the physiological noise will help to improve the ASL CBF quantification stability, though it is not always practical to acquire the physiological signal in routine ASL MRI scans.

Overall, removing global signal fluctuations showed less improvement than removing the residual motions. Although it is difficult to tell how much in the total variance each nuisance accounts for, this difference might reflect a need for a better approach for calculating the global fluctuations. For example, principal component analysis can be used to reduce noise while still keeping the perfusion signal of interest intact [30], so it could be potentially used to estimate the global fluctuations as well.

In summary, both residual motion artifacts and spin labeling fluctuations should be removed before CBF quantification in ASL MRI. To be useful for ASL users, we have provided the implementation of the simplified ASL image motion correction routine in the latest version of ASLtbx, which can be freely obtained through <http://cfn.upenn.edu/~zewang>. The proposed nuisance removal methods will be available in ASLtbx too. Further distribution of these routines through ASLtbx should be of interest to a broad range of ASL users.

## Acknowledgment

This research was supported by NIH grants R01MH080729, R21DC011074, R03DA023496, RR02305, R21DA026114 and R01DA025906.

## References

- [1] Detre JA, Leigh JS, Williams DS, Koretsky AP. Perfusion imaging. *Magn Reson Med* 1992;23:37–45.
- [2] Williams DS, Detre JA, Leigh JS, Koretsky AP. Magnetic resonance imaging of perfusion using spin inversion of arterial water. *Proc Natl Acad Sci* 1992;89:212–6.
- [3] Wong EC. Potential and pitfalls of arterial spin labeling based perfusion imaging techniques for MRI. In: Bandettini CTWMA, editor. *Functional MRI*; 1999. p. 63–9.
- [4] Ye FQ, Berman KF, Ellmore T, Esposito G, Horn JDv, Yang Y, et al.  $H_2^{15}O$  PET validation of steady-state arterial spin tagging cerebral blood flow measurements in humans. *Magn Reson Med* 2000;44:450–6.
- [5] Friston KJ, Williams S, Howard R, Frackowiak RS, Turner R. Movement-related effects in fMRI time-series. *Magn Reson Med* 1996;35:346–55.
- [6] Wang Z, Aguirre GK, Rao H, Wang J, Fernández-Seara MA, Childress AR, et al. Empirical optimization of ASL data analysis using an ASL data processing toolbox: ASLtbx. *Magn Reson Imaging* 2008;26:261–9 PMC2268990.
- [7] Aguirre GK, Detre JA, Zarahn E, Alsop DC. Experimental design and the relative sensitivity of BOLD and perfusion fMRI. *Neuroimage* 2002;15:488–500.
- [8] Liu TT, Wong EC. A signal processing model for arterial spin labeling functional MRI. *Neuroimage* 2005;24:207–15.
- [9] Lu H, Donahue MJ, van Zijl PC. Detrimental effects of BOLD signal in arterial spin labeling fMRI at high field strength. *Magn Reson Med* 2006;56:546–52.
- [10] Wang JJ, Aguirre GK, Kimberg DY, Detre JA. Empirical analyses of null-hypothesis perfusion fMRI data at 1.5 and 4 T. *Neuroimage* 2003;19:1449–62.
- [11] Wang JJ, Wang Z, Aguirre GK, Detre JA. To smooth or not to smooth? ROC analysis of perfusion fMRI data. *Magn Reson Imaging* 2005;23:75–81.
- [12] Chuang KH, van Gelderen P, Merkle H, Bodurka J, Ikonomidou VN, Koretsky AP, et al. Mapping resting-state functional connectivity using perfusion MRI. *Neuroimage* 2008;40:1595–605.
- [13] Tan H, Maldjian JA, Pollock JM, Burdette JH, Yang LY, Deibler AR, et al. A fast, effective filtering method for improving clinical pulsed arterial spin labeling MRI. *J Magn Reson Imaging : JMRI* 2009;29:1134–9.
- [14] Bibic A, Knutsson L, Stahlberg F, Wirestam R. Denoising of arterial spin labeling data: wavelet-domain filtering compared with Gaussian smoothing. *MAGMA* 2010;23:125–37.
- [15] Wells JA, Thomas DL, King MD, Connelly A, Lythgoe MF, Calamante F. Reduction of errors in ASL cerebral perfusion and arterial transit time maps using image de-noising. *Magn Reson Med* 2010;64:715–24.
- [16] Chang C, Glover GH. Effects of model-based physiological noise correction on default mode network anti-correlations and correlations. *Neuroimage* 2009;47:1448–59.
- [17] Desjardins AE, Kiehl KA, Liddle PF. Removal of confounding effects of global signal in functional MRI analyses. *Neuroimage* 2001;13:751–8.
- [18] Fox MD, Raichle ME. Spontaneous fluctuations in brain activity observed with functional magnetic resonance imaging *Nature reviews. Neuroscience* 2007;8:700–11.
- [19] Macey PM, Macey KE, Kumar R, Harper RM. A method for removal of global effects from fMRI time series. *Neuroimage* 2004;22:360–6.
- [20] Wang J, Zhang Y, Wolf RL, Roc AC, Alsop DC, Detre JA. Amplitude-modulated continuous arterial spin-labeling 3.0-T perfusion MR imaging with a single coil: feasibility study. *Radiology* 2005;235:218–28.
- [21] Friston KJ, Ashburner J, Frith CD, Poline J-B, Heather JD, Frackowiak RSJ. Spatial registration and normalization of images. *Hum Brain Mapp* 1995;3:165–89.
- [22] Behzadi Y, Restom K, Liao J, Liu TT. A component based noise correction method (CompCor) for BOLD and perfusion based fMRI. *Neuroimage* 2007;37:90–101.
- [23] Restom K, Behzadi Y, Liu TT. Physiological noise reduction for arterial spin labeling functional MRI. *Neuroimage* 2006;31:1104–15.
- [24] Hernandez-Garcia L, Jahanian H, Rowe DB. Quantitative analysis of arterial spin labeling fMRI data using a general linear model. *Magn Reson Imaging* 2010;28:919–27.
- [25] Wang JJ, Aguirre GK, Kimberg DY, Roc AC, Li L, Detre JA. Arterial spin labeling perfusion fMRI with very low task frequency. *Magn Reson Med* 2003;49:796–802.
- [26] Buckner RL, Andrews-Hanna JR, Schacter DL. The brain's default network: anatomy, function, and relevance to disease. *Ann N Y Acad Sci* 2008;1124:1–38.
- [27] Fox MD, Zhang D, Snyder AZ, Raichle ME. The global signal and observed anticorrelated resting state brain networks. *J Neurophysiol* 2009;101:3270–83.
- [28] Murphy K, Birn RM, Handwerker DA, Jones TB, Bandettini PA. The impact of global signal regression on resting state correlations: are anti-correlated networks introduced? *Neuroimage* 2009;44:893–905.
- [29] Wu WC, Edlow BL, Elliot MA, Wang J, Detre JA. Physiological modulations in arterial spin labeling perfusion magnetic resonance imaging. *IEEE Trans Med Imaging* 2009;28:703–9.
- [30] Hu WT, Wang Z, Lee VM, Trojanowski JQ, Detre JA, Grossman M. Distinct cerebral perfusion patterns in FTL and AD. *Neurology* 2010;75:881–8.